# Field Test of Temporary Excavation Wall Support in Sensitive Clay

**Miah Alam**, *Ph.D. candidate, Department of Construction Engineering, Université du Québec, École de Technologie Supérieure, (Montreal Canada); email: mmaksudulalam@gmail.com*
**Omar Chaallal**, *Ph.D., F.ASCE, F.CSCE, Professor, Department of Construction Engineering, Université du Québec, École de Technologie Supérieure, (Montreal Canada); email: Omar.Chaallal@etsmtl.ca*
**Bertrand Galy**, *Ph.D., Researcher, Dept. of Research, Québec Occupational Health and Safety Research Institute (IRSST), (Montreal Canada); email: Bertrand.Galy@irsst.qc.ca*

**ABSTRACT***: This paper presents the results of a field experimental study carried out to investigate the soil pressure on a temporary flexible trench shoring in sensitive clay. The installation, instrumentation, and field test procedures are presented for two trench boxes "stacked upon each other" in conformity with United States OSHA regulations and placed inside the trench to cover the total 6 m (20 ft) depth of excavation. The field test results are presented in terms of soil pressure distribution along the depth of excavation with and without a 45 kPa surface surcharge next to the edge of one side of the trench. The results reveal the potential use of an existing excavation and trench shoring system in this type of soil and validate its performance with published theoretical results. In terms of soil pressure distribution along the trench, the analytical formulae generally underestimated the experimental values for the type of sensitive clay considered in this study.*

**KEYWORDS:** Field test; Earth pressure; Soft and sensitive clay; Flexible temporary shield; Trench box; Total pressure cells.

**SITE LOCATION: Geo-Database**

## INTRODUCTION

Earth excavation and related trench protection safety for workers are growing concerns worldwide. As a protection system, the trench box shield is different from other shoring systems. The reason is that it is intended not only to shore up or otherwise support the trench face, but to also protect workers from cave-ins or similar incidents inside the trench. Multiple trench boxes can be assembled to create a box system capable of shoring up trenches up to 11 m (35 ft) deep (Macnab, 2002). This system is easy to transport, assemble, and install in narrow trenches. Shields may not be subjected to loads exceeding those that the system can withstand (OSHA, 2015). The earth pressure distribution on a shield depends on the type of soil, the shoring, and the method of implementation. Generally, no satisfactory consensual theoretical solutions are available to estimate soil pressure for this type of supporting structure with partitions facing land pressures in sensitive clay (NBCC, 2015). Many researchers have suggested theoretical solutions to estimate earth pressure on a flexible temporary support. Consequently, for an excavation shield, the Canadian Foundation Engineering Manual (CFEM, 2006) recommends the use of pressure envelopes from empirical data.

Terzaghi and Peck (1967) methods (TPM) for estimating apparent earth pressure are highly popular among practitioners because they are clearly understood and easy to implement. A typical expression is:

$$p_A = 1.0\, K_A \gamma H \tag{1}$$

where $K_A$ is the coefficient of earth pressure, $K_A = 1 - \frac{m4s_u}{\gamma H}$, $\gamma$ is the unit weight of soil, $H$ is the depth of excavation, $S_u$ is the average undrained shear strength value over the height of the wall, and $m$ is an empirical factor accounting for potential base instability effects in deep excavations in soft clays.

Figure 1 shows a diagram proposed by the authors representing apparent earth pressure on a flexible retaining structure in soft to medium clay.
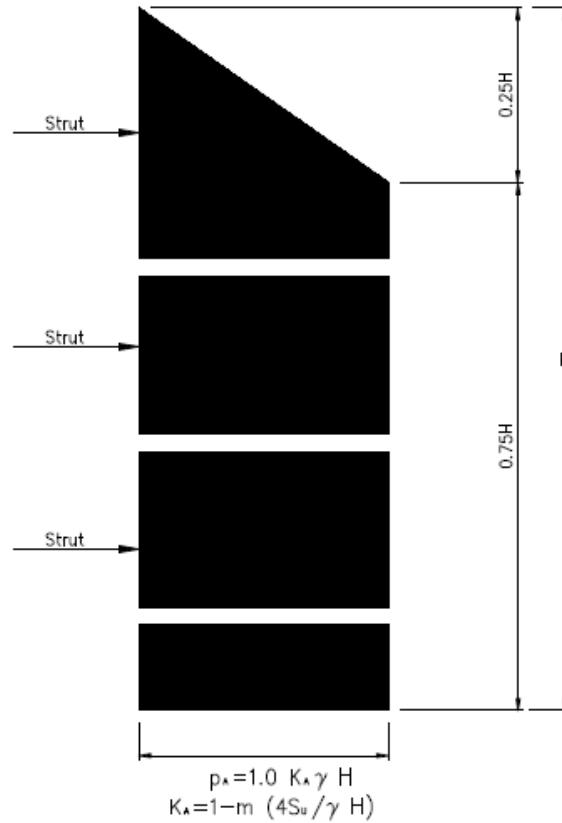


*Figure 1. Apparent earth pressure diagram for soft to medium clay (adapted from Terzaghi and Peck (1967)).*

When the excavation is underlain by deep soft clay and the dimensionless number ($N = \gamma H/S_u$) exceeds 4, then *m* is set to 0.4; otherwise, *m* is set to 1.0 (Flaate, 1966). These formulae are clearly understood and easy to estimate; however, the method does not account for the development of soil failure below the bottom of the excavation. Again, in this method, it was assumed that the distance from the lowest strut to the excavation bottom corresponded to 20% of the excavation depth and that the load on the lowest strut was computed by multiplying the pressure ($p_A$) by half the distance to the strut above plus half the distance below the bottom of the excavation. The total active thrust over the excavation depth on a smooth wall, as suggested by Rankine (1857), is given by:

$$P_{Rankine} = 0.5(\gamma H^2 - 4s_u H) \tag{2}$$

where $\gamma$, $H$, and $S_u$ are as defined above.

On the other hand, to determine the apparent earth pressure for soft to medium clay, Henkel (1971) considered the basal stability phenomena as follows:

$$p_A = \left(1 - \frac{4s_u}{\gamma H} + \Delta K\right)\gamma H \tag{3}$$

where the factor ΔK is related to bottom heave stability as follows:

$$\Delta K = \frac{2B}{H\left(1 - \frac{5.14s_{ub}}{\gamma H}\right)} \tag{4}$$

where B is the width of the excavation and $s_{ub}$ is the average undrained shear strength value below the excavation depth $H$. The distributed horizontal earth pressure (lb/ft$^2$) according to Yokel et al. (1980) can be computed using the following equation:

$$p = We\,(H + 2) \qquad (5)$$

where $We$ = lateral weight effect (lb/ft$^3$) and $H$ = height of the supported bank (ft) (2 ft are added to allow for overloading) (Note: 1 lb/ft$^2$ = 48 Pa). The above discussion reveals that calculating earth pressure on a flexible retaining structure is not straightforward and that various soil parameters must be evaluated and considered when designing or validating a shoring system in a soft clay excavation or trench (Yokel et al., 1980).

This study presents a full-scale field test investigation at a unique site made exclusively of soft, sensitive clay soil and located in Louiseville, Quebec, Canada, to evaluate the earth pressure on an excavation with temporary flexible shoring. The trench was 6 m deep, and the shoring consisted of two steel trench boxes stacked upon each other. The field test results are presented in terms of soil pressure with depth of soil. This paper provides a detailed explanation of the installation phase, including instrumentation, and the test phase. The experimental results are presented and compared with available Rankine (1857), Terzaghi and Peck (1967), and Yokel (1980) theoretical apparent earth pressure values and available field performance data reported by LaBaw (2009).

## FULL-SCALE FIELD EXPERIMENTAL PROGRAM

To meet the objectives related to the evaluation of earth pressure and the performance validation of a temporary shield system, an experimental trench was excavated and an excavation protection system set up at the field test site located in Louisville, Quebec.

### Soil Characteristics of the Field Experimental Site

The field experimental site is located about 100 km north-east of Montreal, on the north shore of the St. Lawrence River. It is along Highway 138, 8 km west of Louiseville village. The elevation of the site is 9.5 m above sea level. The site is known for its so-called sensitive clay soil, and therefore it was selected for the present study. The soil is made up of a 60 m-thick, Champlain Sea high-plasticity clay deposit (Leblond, 1981). According to Leroueil et al. (2003), this clay is extremely homogeneous, with 80% clay fraction, 45% average plasticity index, and an average sensitivity (St) of 22 (as determined with the Swedish fall cone).

Experimental shear tests were performed by Laval University (Quebec City) in the field using a scissometer (Roctest model M-1000). Dourlet (2020) describes the characterization tests conducted on this site. Figure 2 shows the shear strength data for undrained soil at the Louiseville experimental site, the soil layers, Atterberg limits, and effective stresses. The preconsolidation stress was obtained from the oedometer consolidation test using Casagrande's technique. The overconsolidation ratio (OCR) was computed as the effective preconsolidation pressure obtained from the oedometer test divided by the *in-situ* effective overburden pressure. The average volumetric weight measured was 14.8 kN/m$^3$ (varying from 14.60 to 14.97 kN/m$^3$ depending on sample depth).

Soil samples were obtained with the large-diameter Laval tube sampler (200 mm diameter, 600 mm height), which has been specifically developed for sensitive clays (Rochelle et al., 1981). Four soil samples (tubes) were obtained at two different depths: two tubes from 2.13 m to 2.73 m depth, and two tubes from 3.05 m to 3.65 m depth. The shear strength profile with depth is very similar to the shear strength profile obtained by Leroueil et al. (2003) for Louiseville sensitive clay on the same test site. A comparison of geotechnical parameters for this test site is presented by Dourlet (2020). DSS testing was conducted on soil samples corresponding to 3.05 to 3.65 m depth (two samples retrieved on site). Three DSS tests were conducted on 3.47 m depth samples, under static loading, at a constant volume, but different effective vertical stresses.

The details and results of these three tests are summarized in Table 1. Two of them were undertaken in the overconsolidated domain and one in the normally consolidated domain. In the overconsolidated domain, DSS$_{stat}$-01 showed a contraction behavior, whereas DSS$_{stat}$-02 showed a slight dilation behavior. In the normally consolidated domain, DSS$_{stat}$-03 showed a contraction behavior. Effective stress parameters obtained from DSS tests are presented in Table 2. These parameters can be useful for modeling the long-term behavior of the trench. They are comparable to data published by Lefebvre (1981) for

Champlain Sea clays, which are a common type of sensitive clay in the Province of Quebec. Extensive characterization and testing of the Louiseville clay (same test site) are presented in Leroueil et al. (2003).
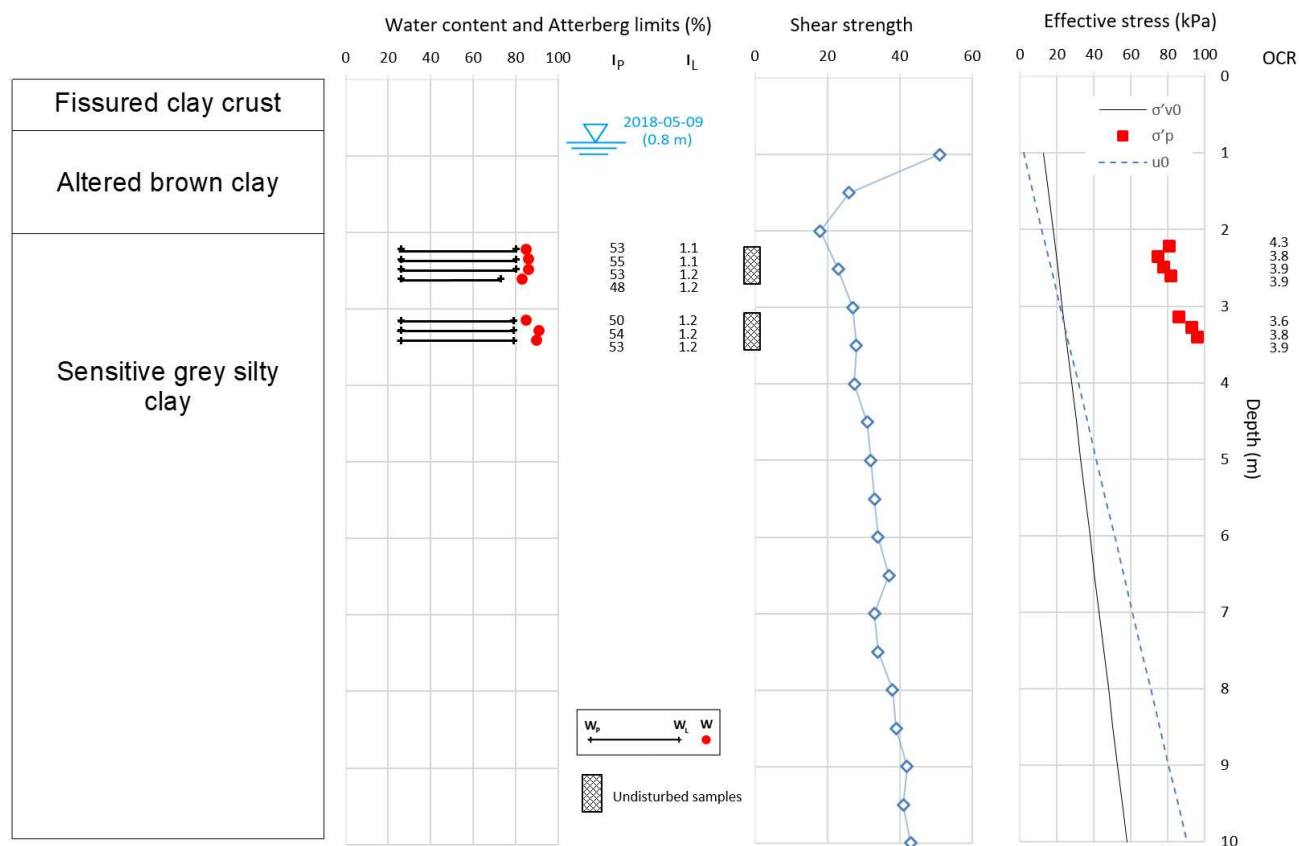


*Figure 2. Geotechnical properties of Louiseville clay deposit (Data adapted from Dourlet 2020).*

*Table 1. Undrained shear strength form the soil based on DSS testing (data from Laval University).*

| Test | Consolidation | | Initial rupture | | Large deformations | |
|---|---|---|---|---|---|---|
| | $\sigma'vc$ (kPa) | $e_C$ | $S_u$ (kPa) | $\gamma h$ (%) | $S_{u-gd}$ (kPa) | $\gamma h$ (%) |
| DSS$_{STAT}$-01 | 57 | 2.287 | 28 | 2.3 | 23 | 15 |
| DSS$_{STAT}$-02 | 25 | 2.290 | 20 | 2 | 22 | 15 |
| DSS$_{STAT}$-03 | 143 | 1.804 | 40 | 5 | 36 | 15 |

*Table 2. Effective stress parameters from DSS testing (data from Laval University).*

| Domain | DSS tests |
|---|---|
| Over consolidated domain | c' = 9 kPa |
| | $\phi$' = 28° |
| Normally consolidated domain | c' = 0 kPa |
| | $\phi$' = 26.5° |

**Excavation and Shoring Geometry**

The trench box system used is illustrated in Figure 3, and the geometric and mechanical properties of the trench box are summarized in Table 3. This "cage-type shield" or "trench box" is a very common protection system in the construction industry. The excavated area between the outside of the trench box and the face of the trench should be as small as possible (OSHA, 2015). Considering this recommendation, the contour of the excavation considered in this experiment was 5.59 m (18.33 ft) long and 2.18 m (7.15 ft) wide, accommodating the trench box that was 3.05 m (10 ft) long, 1.75 m (5 ft) wide, and 6 m (20 ft) deep (see Figure 4(a)). Two trench boxes "stacked upon each other" in conformity with the OSHA (2015) procedure were placed into the trench excavation as shown in Figure 4(b) to cover the total depth of excavation, 6 m (20 ft), and to act as one protection system because they were assembled to each other using "hinge" connections.
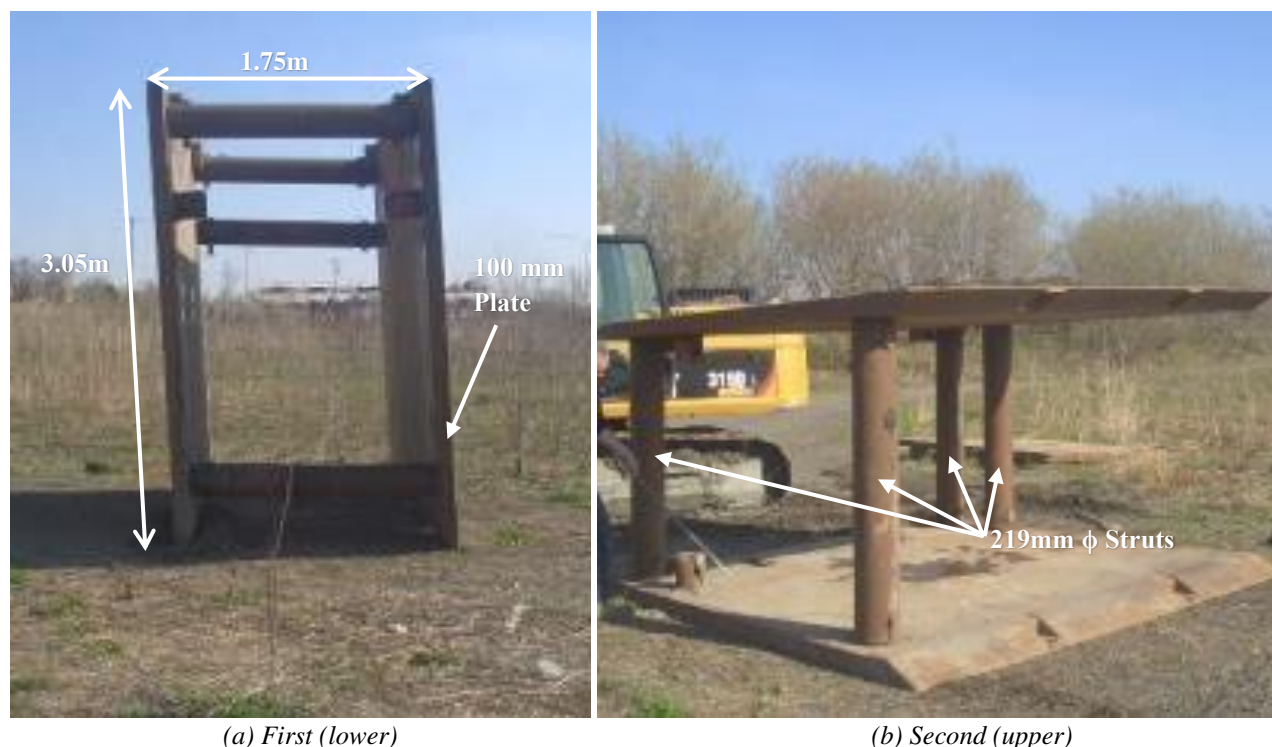


<div align="center">

*(a) First (lower)*          *(b) Second (upper)*

*Figure 3. First and second steel trench box protection system at the experimental site.*

*Table 3. Geometric and structural properties of the shield.*

</div>

| Properties (one-shield geometry) | Steel trench box |
| --- | --- |
| Length, m (ft.) | 3.05 (10) |
| Height, m (ft.) | 3.05 (10) |
| Thickness of the plate, mm (in.) | 100 (4) |
| Strut or spreader tube outer diameter, mm (in.) | 219 (8.61) |
| Strut or spreader tube inner diameter, mm (in.) | 194 (7.63) |
| Cross-sectional area of strut, $m^2$ ($in^2$) | 8.24E-03 (12.77) |
| Strut or spreader tube moment of inertia, $m^4$ ($in^4$.) | 4.41E-05 (106) |
| Modulus of elasticity for plate and strut, $kN/m^2$ (ksi) | 2.00E+08 (29007) |
| Shear modulus, $kN/m^2$ (ksi) | 8.00E+07 (11603) |
| Poisson's ratio | 0.30 |

**Instrumentation**

Table 4 shows the identification and capacities of the pressure cells installed on the trench box before its installation. Five vibrating-wire pressure cells (model TPC) were used to capture soil pressure at the following soil depths from the top of the

steel trench box: 0.9 m, 2.4 m, 2.4 m, 3.9 m, and 5.4 m. At 2.4 m depth, a pair of cells was used to capture to what extent/scale the pressure varied beyond the centerline of the trench box. The locations of the pressure cells attached to the trench box for the purpose of the test are shown in Figure 4(c), and the locations of the struts are shown in Figure 5. Pressure cells were installed on only one of the two sides of the trench box. In this experiment, pressure cells were attached on one side, as shown in Figure 4(c). The other two sides were open to the soil along the trench, as shown in Figure 4(b). Note that the horizontal distance between struts was 2.64 m.
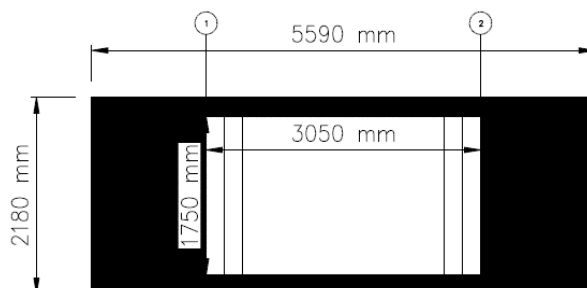
*(a) Plan view of trench.*
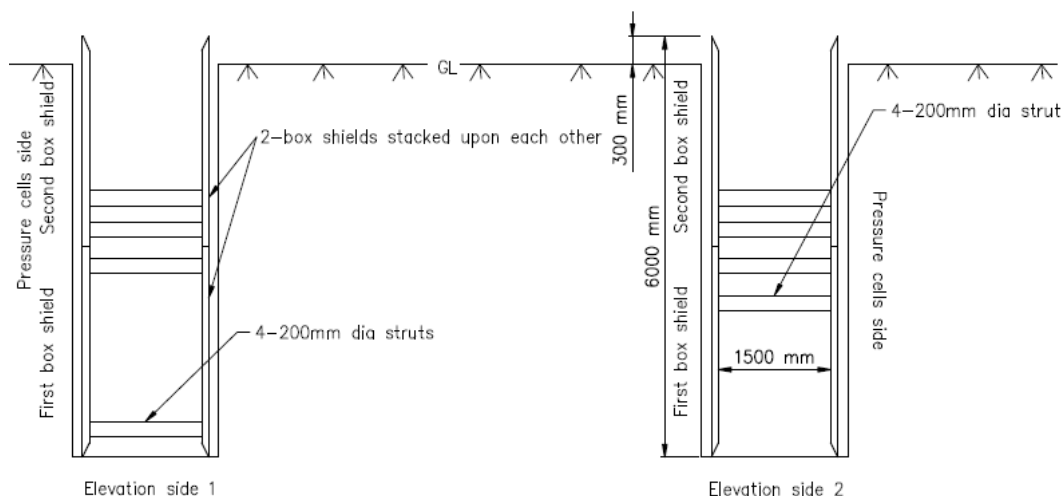
*(b) Elevation views of trench and trench boxes.*
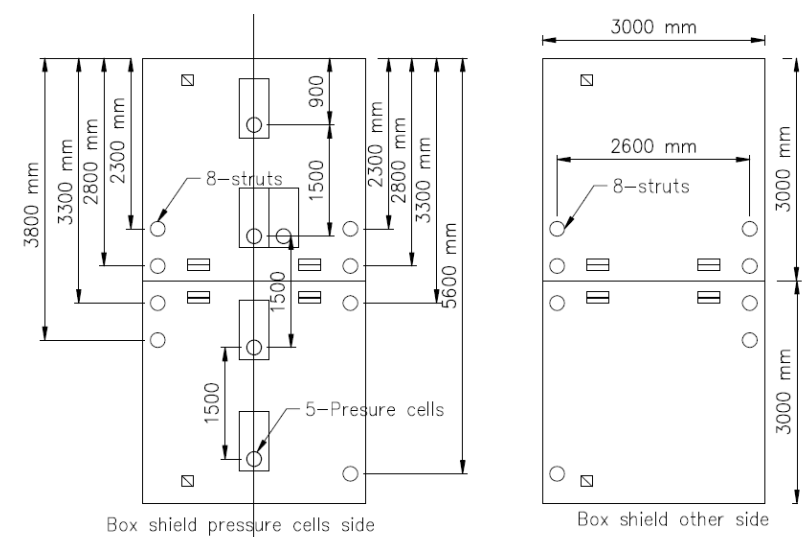
*(c) Strut spacing and location on the two walls of the trench box.*

*Figure 4. Field test setup details for trench boxes.*

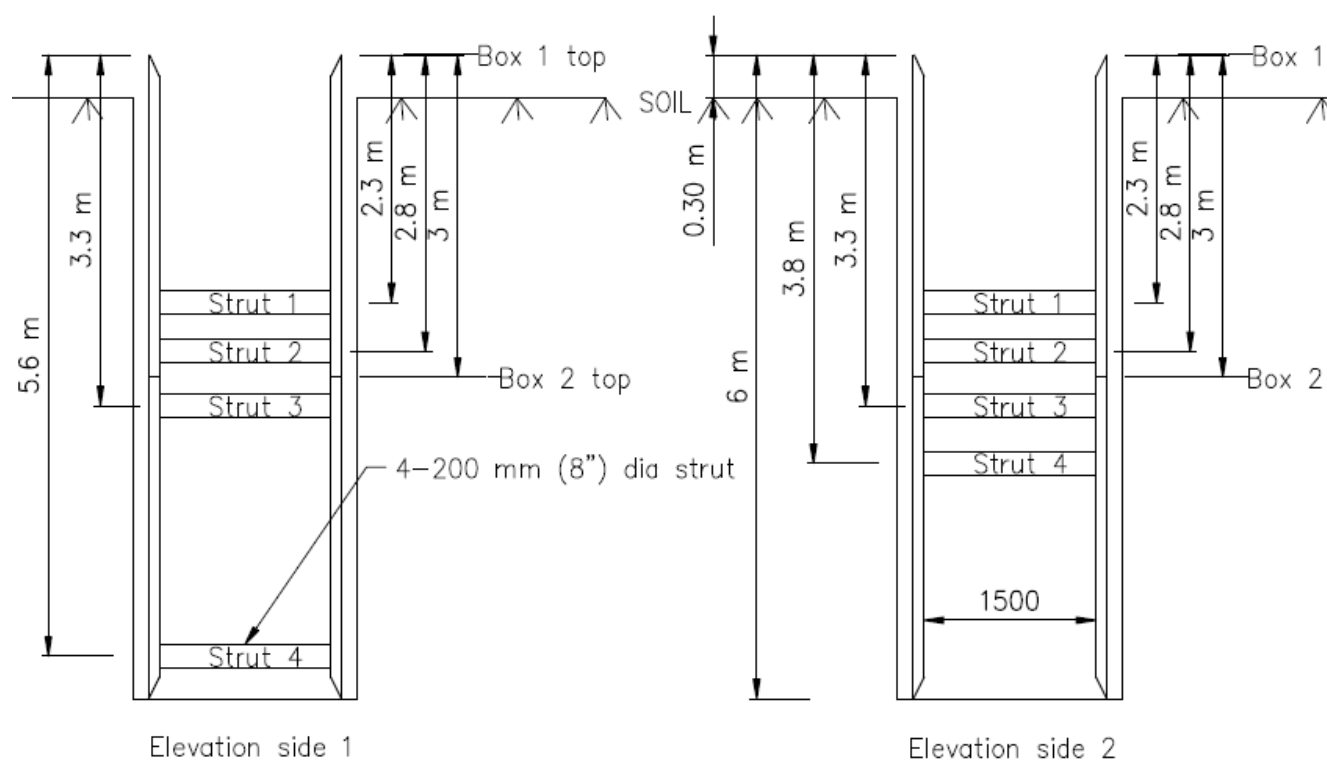| Pressure cell identification | Capacity (kPa) |
|---|---|
| B-P1 | 200 |
| B-P2 | 200 |
| B-P3 | 70 |
| B-P4 | 70 |
| B-P5 | 70 |



*Figure 5. Strut locations in the two elevation sides along the trench.*

**Laboratory Verification and Field Installation of Test Equipment**

The pressure cells were first individually attached to plywood frames 19 mm thick with epoxy at the ETS laboratory, as illustrated in Figure 6(a). Two main reasons justified this initiative: (i) to ensure the surface receiving the cells was plane (the trench box plate was neither flat nor smooth enough), and (ii) to optimize the time required to attach the pressure cells to the trench box at the experimental site (an open field). After all the pressure cells were bonded to the plywood surface, they were carefully tested in the laboratory to check their functionality under pressure before they were transported to the experimental site (Figure 6(b)). For this purpose, the pressure cells were connected individually with the Roctest SENSLOG 1000X datalogger (a turnkey system used for the remote monitoring of virtually any type of instrument), and loads were applied gradually in the structural test laboratory at ETS (Figure 6(c)).

Note that calibration of the pressure cells was undertaken by the equipment provider and that a calibration document was supplied with the equipment. For pressure cells B-P1 (at 5.4 m) and B-P2 (at 3.9 m), the 0-200 kPa pressure range was used for calibration, whereas for B-P3 (at 2.4 m), B-P4 (at 2.4 m), and B-P5 (at 0.9 m), the 0-70 kPa range was used. Because the deeper part of the trench experienced more pressure compared to the upper part, two 200-kPa capacity pressure cells were used in the deeper part (approximately twice the expected earth pressure at 5.4 m), and three 70-kPa capacity pressure cells were used in the upper portion (approximately twice the expected earth pressure at 2.4 m). Details of the pressure cells are provided in Figure 4(c) and Table 4. Once all the pressure cells had been verified as functional in the laboratory, they were

transported to the experimental site. Vibrating wire pressure cells (model TPC) are reliable, faster than all other types, and almost immune to external noise because they rely on the frequency output (Roctest, 2005). A previous experimental study by Lan et al. (1999) successfully used this type of pressure cell to measure the apparent earth pressure.
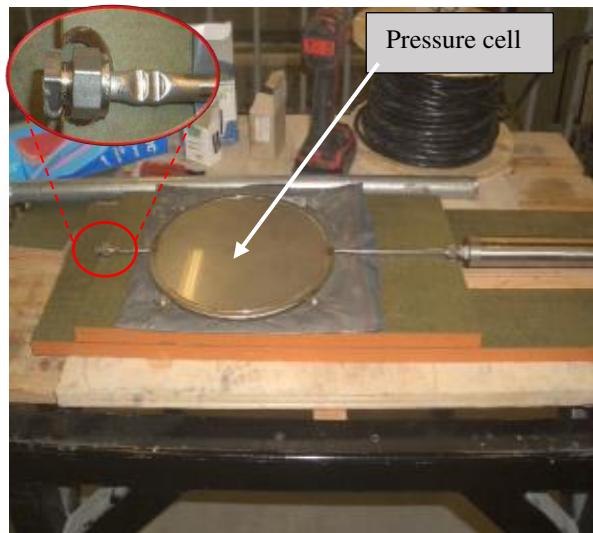


*(a) Pressure cell was attached to the plywood.*
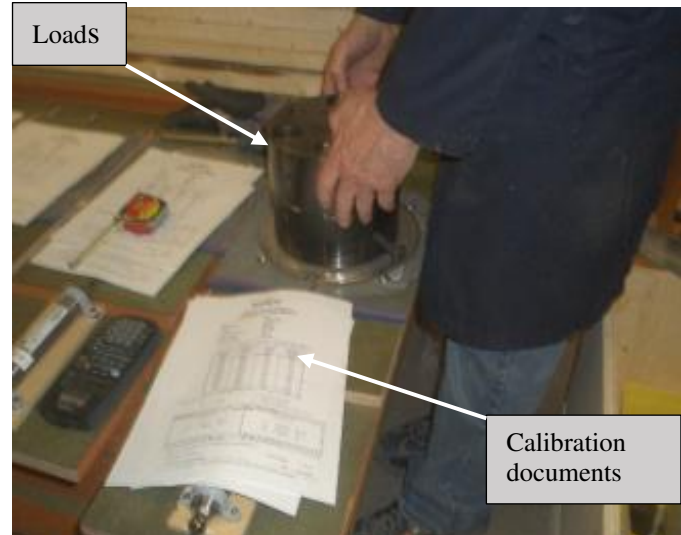


*(b) Loads were placed on the pressure cell to check its functionality.*



*(c) Pressure cells were verified by the SENSLOG datalogger in the ETS lab before site installation.*



*(d) Sufficient sensor cables were attached to each pressure cell for extra length if required to connect with the SENSLOG.*

*Figure 6. Preparation and verification of pressure cells in the ETS lab before being transported to the site installation.*

To install the pressure cells on the steel wall plate of the trench box, the following steps were undertaken: (i) the box steel wall plate surface was identified and prepared, and then epoxy was used on both the steel and the plywood surfaces as illustrated in Figure 7; (ii) the plywood holding the pressure cells was attached to the steel wall plate surface; and (iii) to further secure the connections, the plywood was screwed into the steel wall plate as illustrated in Figure 8.
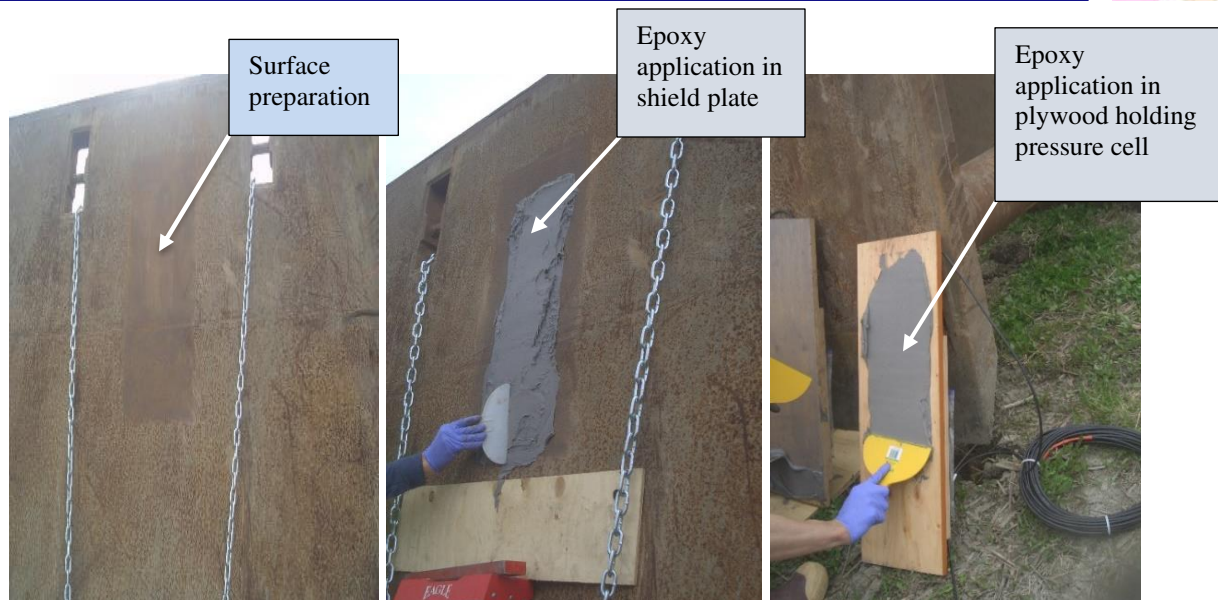
Surface preparation

Epoxy application in shield plate

Epoxy application in plywood holding pressure cell

*Figure 7. Steps to install the pressure cells on the steel wall plate of the trench box.*



Attached pressure cells in the 1st part of protection shield

Attached pressure cells in the 2nd part of protection shield

*Figure 8. Pressure cells are fixed on the side of the first and second trench boxes.*

**Excavation and Installation of Protection Systems**

The field tests were performed in 2018 from May 14 to August 8 without surcharge loading, and from August 8 to August 10 with a 45 kPa surcharge load consisting of concrete blocks. After all the pressure cells had been bonded to the wall steel plate of the two trench boxes, the top soil (with surface vegetation) was removed from the trench zone. Using an excavator, the trench was excavated to approximately 1.5 m depth from the top, and the first (lower) trench box was installed rapidly to make sure that the surrounding soil would not fall inside the trench, as shown in Figures 9 to 12 which illustrate the excavation sequence. Thereafter, excavation through the trench box continued gradually until reaching 6 m depth, and the first (lower) box was pushed down to accommodate the second (upper) box, as depicted in Figure 11. Finally, the second (upper) trench box was installed on top of the first box as per OSHA guidelines for shields "stacked upon each other," and the two boxes were assembled using the four "hinge" connections located in the four corners, as shown in Figure 12.

A space between the trench box exterior wall and the surrounding soil ranging from 100 mm to 200 mm was created due to the installation process. OSHA (2015) states that, "the space between the trench boxes and the excavation side is backfilled to prevent lateral movement of the box." Therefore, after successfully installing the boxes one on top of the other, the empty

space between the retaining (shoring) exterior wall and the surrounding soil was backfilled with sand, as shown in Figure 13. In addition, the height between the trench box top and the soil surface was kept to 300 mm on both sides (Figure 13) in compliance with the SCCI (2020) recommendation that "the shoring shall extend 300 mm above the excavation." Finally, the two open ends of the trench were closed by inserting 10 mm-thick sheet piles, thereby preventing loose soil from falling inside the excavation (Figure 14).
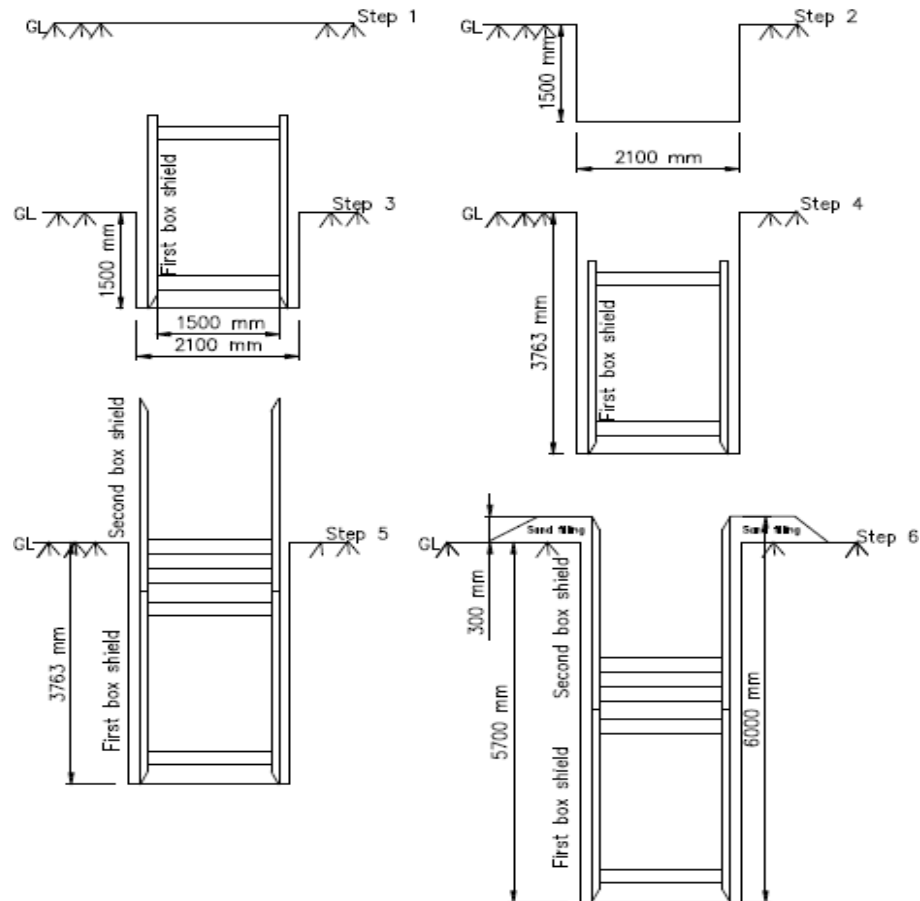


*Figure 9. Excavation/construction sequence.*



*Figure 10. Installation of the first (lower) trench box into the trench.*

*Figure 11. Excavation continued to make room to accommodate the second (upper) trench box in the trench.*



*Figure 12. Second (upper) trench box is being placed on top of the first (lower) box in the trench.*



*Figure 13. Sand was used to fill the space between the shoring exterior wall and the surrounding soil.*

*Figure 14. Concrete blocks (surcharge load) installed on one side of the trench.*

**Concrete Block (Surcharge Load) Installation**

A surcharge load of 45 kPa was applied on one side of the trench using 2.44 m × 0.6 m × 0.6 m concrete blocks during the period from August 8 to 10, 2018, as illustrated in Figure 14. The aim of this loading on the surface of the protection system was to examine the movement of the soil as well as the pressure increase due to the overload. The SCCI standard specifies 1.2 m (4 ft) distance from the excavation (SCCI, 2020). However, OSHA (2015) states that temporary spoil must be placed no closer than 0.61 m (2 ft) from the surface edge of the excavation and that permanent spoil should be placed at some distance from the excavation. In consideration of all these statements, the overload was placed close to the wall to simulate the most unfavorable case.

**Data Recording Unit and Data Collection**

All the sensor cables attached to the pressure cells were brought into the small data acquisition trailer and connected to the appropriate box to record the field test data. Figure 15 shows the small truck trailer chamber that was used at the experimental site to record the test data in real time during the field experiment. All the pressure cells were connected to the central sensor box by sensor cables. Real-time data were collected using Wi-Fi technology from ETS through a dedicated website of the equipment provider.

*Figure 15. Components of the data recording unit at the experimental site.*

**Data Preparation**

ETS had access through the file transfer protocol (FTP) to the website at any time (24/7) to check and collect data. To reduce their volume, the data were recorded at intervals of 30 minutes, 24/7. These data were recorded in the form of raw data such as linear units and Hertz, not directly in kilopascals (kPa) for the pressure cells. Therefore, it was necessary to transform the raw data into an appropriate engineering format using the linear equation recommended by the Roctest (2005) instruction manual related to vibrating-wire total pressure cells. This equation was used as follows for each of the pressure cells separately:

$$P \ = \ C_f \ (L - L_0) \tag{6}$$

where $P$ = pressure in kilopascals (kPa); $C_f$ = calibration factor (provided on calibration sheets for each pressure cell separately); $L$ = current reading in linear units (LU); and $L_0$ = initial reading in linear units (LU). Roctest (2005) also provides a more complex polynomial method. However, the linear method is simpler and easier to use, and the maximum error rate was only 0.23% in the present case.

Next, a correction was applied to take temperature changes into account using the following equation recommended by Roctest (2005):

$$Pc \ = \ P \ - \ C_T(T - T_0) - \ (S - S_0) \tag{7}$$

where $P_C$ = corrected pressure in kPa; $P$ = pressure previously calculated in kPa; $C_T$ = calibration factor for temperature (given in the calibration sheet), in kPa/°C; $T$ = current temperature reading in degrees Celsius; $T_0$ = initial temperature reading in degrees Celsius; $S$ = current barometric pressure reading in kPa; and $S_0$ = initial barometric pressure reading in kPa. The correction factor for barometric reading expressed in the above equation by the term $(S–S_0)$ was neglected, given its tiny value compared with the pressure measured at depth. All the above equations were used to calculate the earth pressure in the trench using Excel worksheets.

## FIELD TEST RESULTS AND DISCUSSION

### Temperature Effect

Figure 16 shows the daily temperature at different trench depths as captured by the pressure cells during the first week. The air temperature is also provided for comparison. The figure reveals that the day-versus-night fluctuations of soil temperature were more significant in the upper pressure cells (B-P5, B-P4, B-P3) than in the deeper pressure cells (B-P1, B-P2) in the trench. The uppermost cell (B-P5) experienced minimum and maximum temperatures of 7°C and 23°C in the first week of the experiment, but the next lower pressure cells (B-P4, B-P3) experienced minimum and maximum temperatures of 9°C and 17°C. Temperature fluctuations were negligible in the deeper pressure cells (B-P1, B-P2).
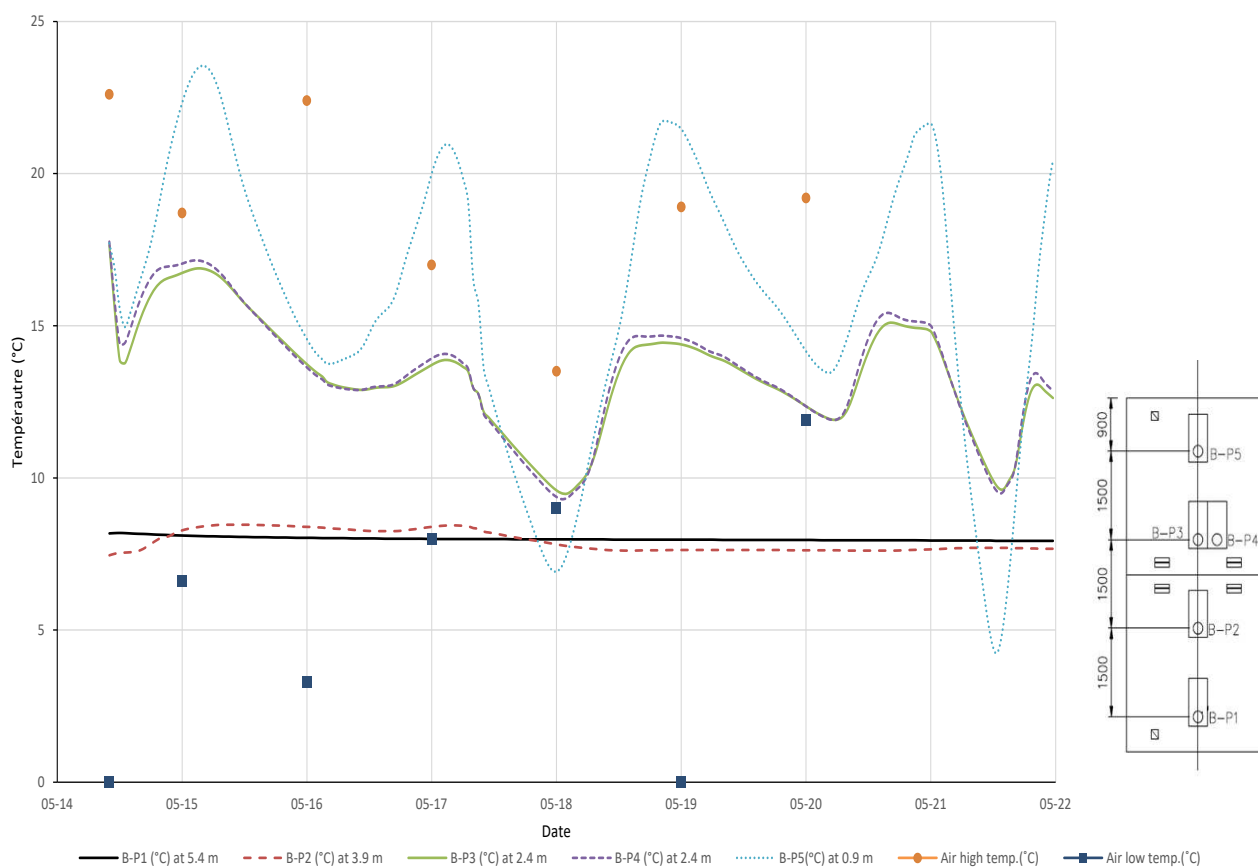


*Figure 16. First week's hourly temperature at different trench depths as recorded by pressure cells, 2018.*

### Soil Pressure over the Time Period (May 14–August 10, 2018)

From Figures 17, 18, and 23, the following observations can be made:

- The calculations revealed that the temperature correction did not result in major differences in soil pressure. Figure 17 presents the recorded hourly soil pressure after temperature correction for the first week (May 14 to 22). It shows how the soil pressure varied with depth during this period. The deeper pressure cells (B-P1, B-P2) experienced higher

values in kPa than the upper pressure cells (B-P5, B-P4, B-P3). Note that the pressure cell at 3.9 m (B-P2) depth recorded higher values in kPa than the cell at 5.4 m (B-P1) depth. However, this can be attributed to the type of trench box used, with fixed end support (Lan et al., 1999).

- Before May 15, the pressure cells experienced higher pressures. However, these higher pressures eased after water that had accumulated in the excavation was pumped out.

- After the trench box was placed in the trench, the negative initial pressure value recorded by pressure cell P5 (0.9 m) was attributed to an artificial effect caused by deflection of the sandwich wall on the outer plane of the shield. One side of the wall was exposed to the sun, resulting in a significant day-to-night temperature variation.

Figure 18 presents the maximum daily pressure curves after temperature correction at different soil depths from May 14 to August 10, 2018 (i.e., up to the last day of the experiment). Examination of the curves reveals various phenomena that occurred during the period of the experiment:

- Soil pressures at depths 0.9 m (B-P5) and 2.4 m (B-P4, B-P3) increased gradually.

- The increase in soil pressure at depth 3.9 m (B-P2) was more pronounced than at depth 5.4 m (B-P1). This is attributed to the fact that the bottom end part of the trench box (approximately 300 mm) was embedded into the soil and that the total gravity load of the upper steel trench box was pushing the lower trench box into the ground during the installation process. Thereby the bottom part (approximately 300 mm) of the lower trench box acted more likely as a "fixed end support" (Figure 23).

- Overall soil pressure increased with depth except for the bottom part of the support, which experienced less pressure than the middle part due to the arching effect. With the embedment of the bottom part of the trench box, the soil around the trench box developed an "arching effect," leading to higher apparent earth pressure just above the bottom of the trench. This phenomenon of nonlinear active earth pressure distribution for flexible retaining structures has been recognized and discussed by numerous authors, including Karlsrud and Andresen (2005), Hashash and Whittle (2002), Mortensen and Andresen (2003), Benmebarek et al. (2016), and Bjerrum et al. (1972).

**Surcharge Load Effect on Soil Pressure**

Figure 19 presents a magnified view of the last week of soil pressure versus depth to evaluate the effects of the overload (concrete blocks) applied near the trench. As expected, soil pressure at depth 2.4 m (B-P4, B-P3) increased rapidly. This contrasts with the minor overload effects observed at depths 3.9 m (B-P2) and 5.4 m (B-P1). Note that the pressure cell at depth 0.9 m (B-P5) recorded almost constant pressure throughout the last week. This can be attributed to the fact that the surrounding soil had been washed away due to heavy rainfall. It can be concluded that the effect of overload was generally more noticeable on the upper part of the trench box than on the lower part. This can also be seen in Figure 20, where the effect of the surcharge load was captured by pressure cells B-P2 and B-P3.

**Total Pressure Curve**

From Figures 20, 21, and 22, the following observations can be made:

- Figure 20 presents the absolute maximum soil pressure versus soil depth at the trench excavation with and without surcharge loading. Experimental values were developed based on experimental field test results (from May 14 to August 10, 2018). The soil pressures at depths 0.9 m (B-P5), 2.4 m (B-P4, B-P3), and 3.9 m (B-P2) were observed to increase rapidly.

- In contrast, the soil pressure at 5.4 m (B-P1) did not show a significant increase, probably due to end boundary conditions (more likely "fixed end support").

- This anomaly can also be explained by other observations. At the beginning of August 2018, it was discovered that the surrounding soil at the pressure cell at 0.9 m depth (B-P5 on the curve) had been totally washed away (Figure 21)

due to heavy rainfall. Informatively, the precipitation quantities for each month during the test period (May to August 2018) are presented in Figure 22.

- Consequently, the pressure cell at 2.4 m depth (B-P3 on the curve) seems to have had less soil above it, resulting in less pressure than expected.

- The pressure cell at 3.9 m depth (B-P2 on the curve) gave the maximum value of soil pressure (114 kPa), which is the expected order of magnitude for this type of experimental excavation trench depth. Using the Plaxis software, Karlsrud and Andresen (2005) computed an apparent earth pressure of 75 to 100 kPa at 4 m depth for a sensitive clay. In an experimental field test performed in silty sand in the urban region of Quebec, Lan et al. (1999) recorded an apparent earth pressure of 113 kPa on a trench box at 3.04 m depth, which is of the same order of magnitude as the pressure at 3.9 m depth obtained at the Louiseville field site in the present study.

- At 5.4 m depth, the pressure cell (B-P1) experienced less pressure because the wall of the trench box was inserted approximately 300 mm (12 in) into the soil, as illustrated in Figure 23, developing thereby a "fixed end support" system, as explained earlier. Therefore, the pressure cell at 5.4 m depth (B-P1) was not able to record the expected pressure without the interference of the so-called "fixed end support."
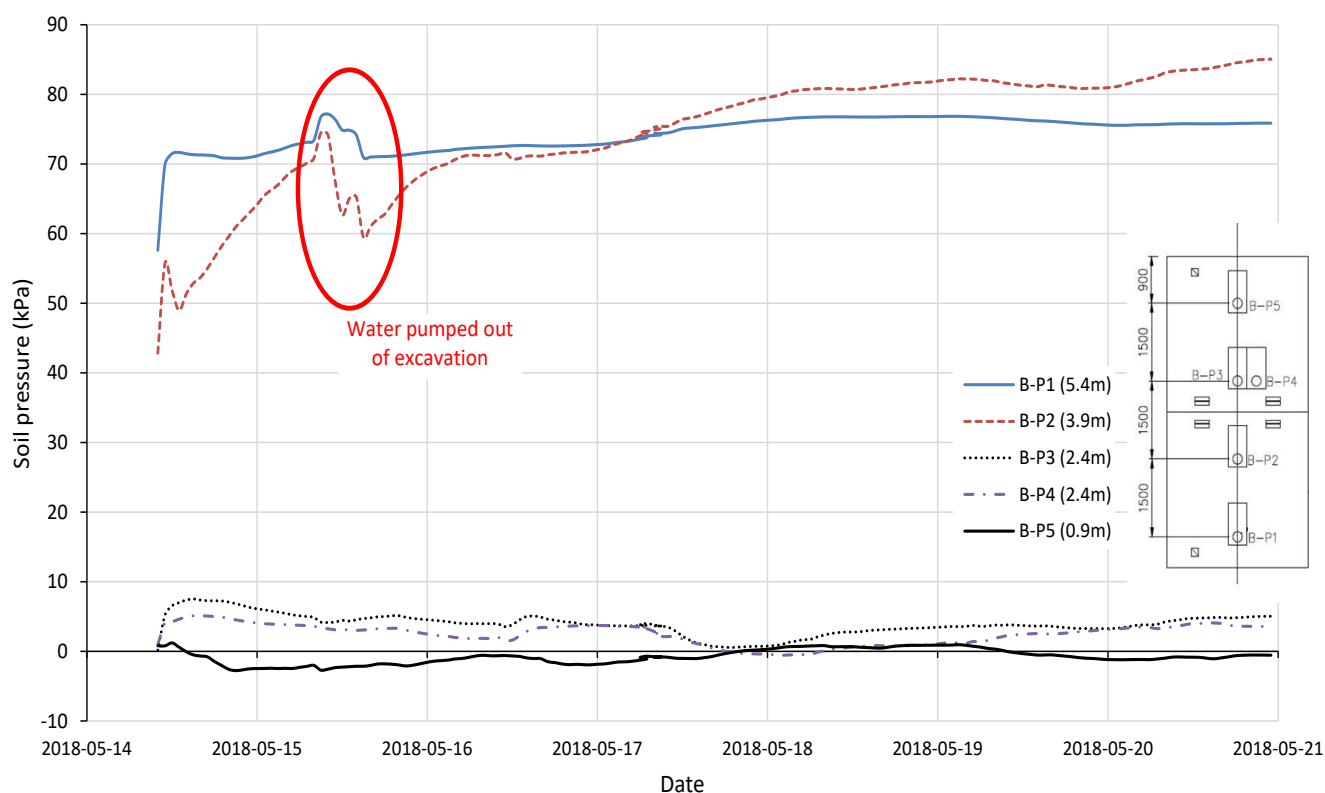


| Initial pressure reading deducted | | | | | |
|---|---|---|---|---|---|
| Pressure cell # | B-P1 | B-P2 | B-P3 | B-P4 | B-P5 |
| Initial reading (kPa) | 20.12 | 23.55 | 6.52 | 10.84 | 6.41 |

*Figure 17. First week's hourly pressure after temperature correction on the trench box protection, 2018.*
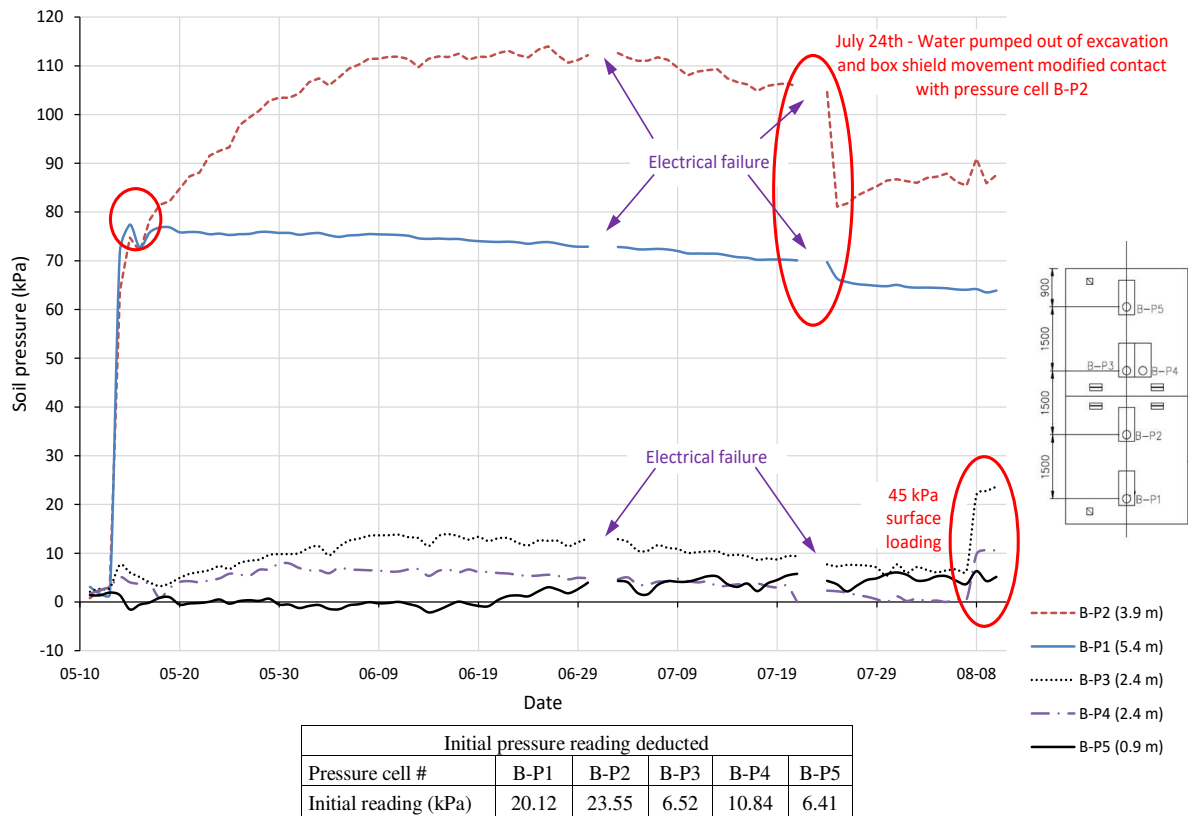
*Figure 18. Maximum daily soil pressure after temperature correction on the trench box protection (May 14–August 10, 2018).*
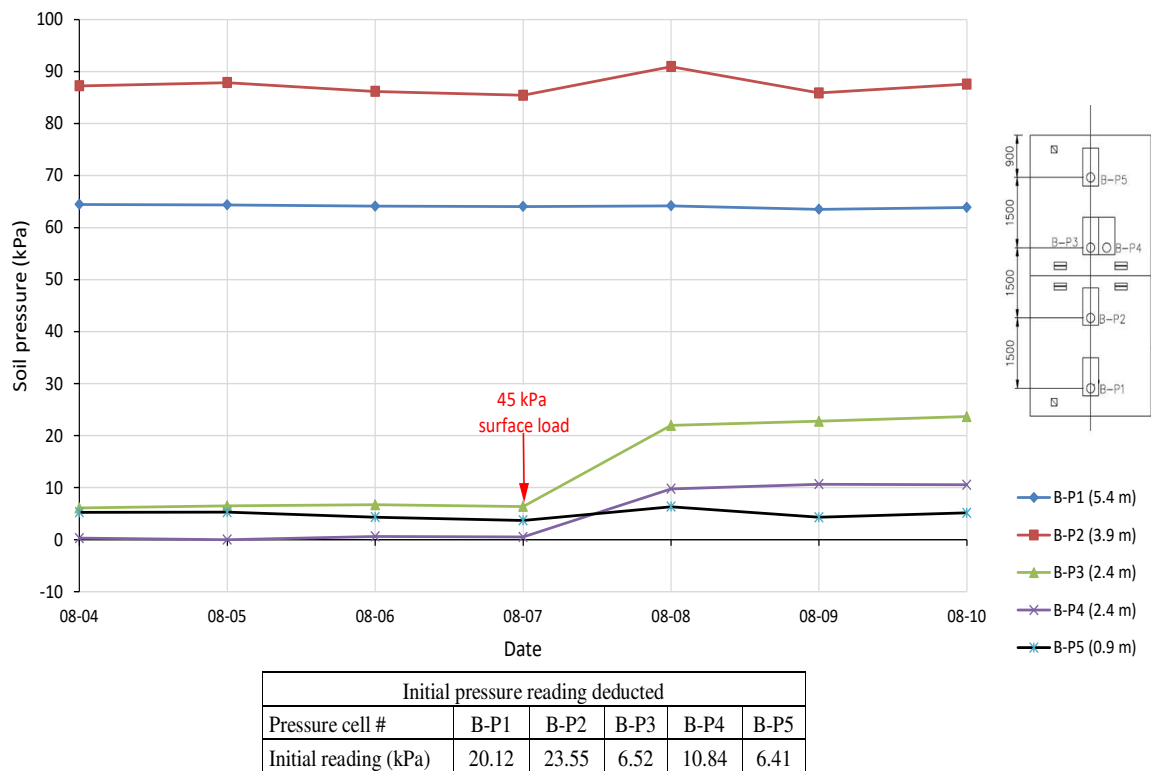


*Figure 19. Blown-up view of the last week of soil pressure to observe the effects of surcharge loading (concrete blocks) at the trench.*
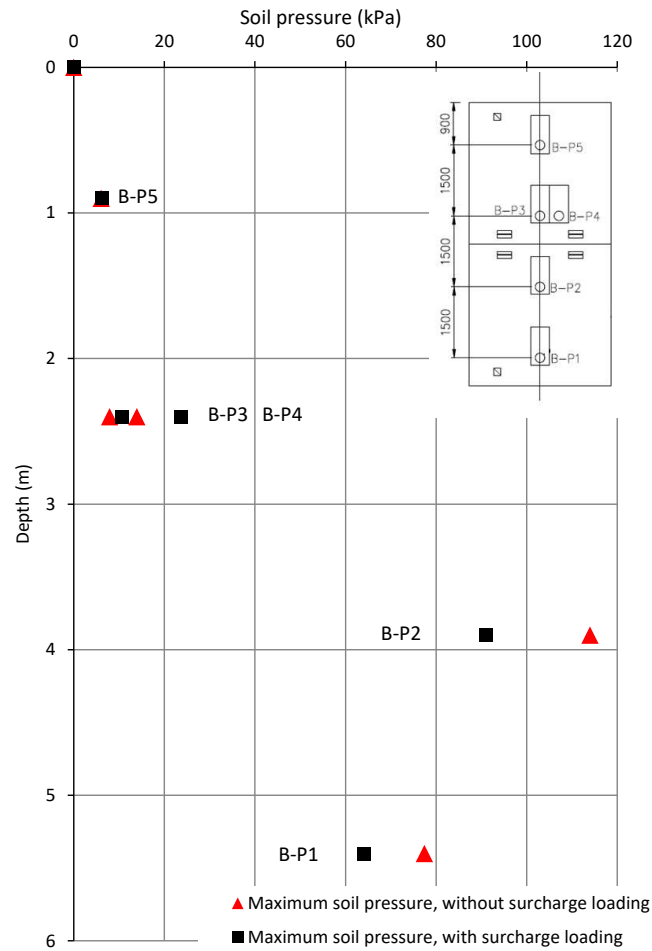
*Figure 20. Experimental soil pressure on trench box wall vs. depth.*



Pressure cell B-P5(at 0.9m depth)

Gap due to soil washed away (created by water flow through this path down due to seasonal rainfall from May to August 2018 in the site).

*Figure 21. Surrounding soil washed away by heavy rainfall affecting pressure cell at 0.9 m.*
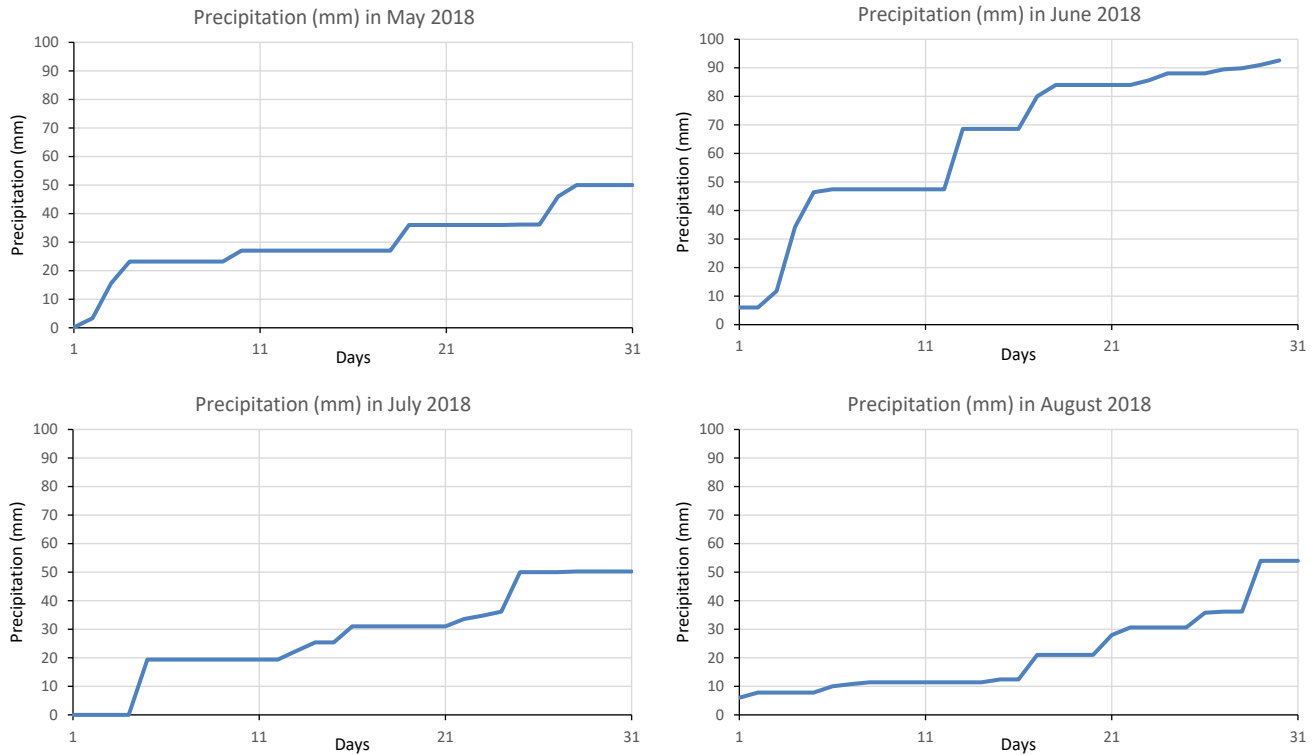
*Figure 22. Recorded accumulated precipitation quantities (in mm) for each month from May to August 2018 at the Louiseville field test site.*



*Figure 23. Likely "fixed end condition" developed at the lower end of the first trench box due to 300 mm insertion into the soil.*

**Theoretical Calculations**

The calculations presented in this section are intended to compare theoretical soil pressure with field test results. Classical theoretical calculations such as the Rankine model and TPM are reasonably accurate to predict apparent earth pressure on flexible retaining structures (such as sheet piles, lagging, etc.), but are not accurate enough for multi-strutted shoring systems such as the trench box used in this study (Macnab, 2002).

According to the TPM equation (1) and Figure 24, the apparent earth pressure for soft clay in the Louiseville soil case is $p_A$= 44 kPa, with $K_A = 1-m(4S_u/\gamma H) = 0.48$. Active earth pressure formulae developed by Rankine (1857) and Yokel et al. (1980) were also used to calculate theoretical soil pressure; the results are summarized in Table 5. The maximum experimental strut loads from field performance data recorded in the LaBaw (2009) study (with $\gamma$ =18.6 kN/m$^3$ and PI = 7.04 for medium clay) are also provided for comparison in the same table. Calculated theoretical and field performance soil pressures for soft clay soil are compared at different depths of the trench in the present study in Figure 25.
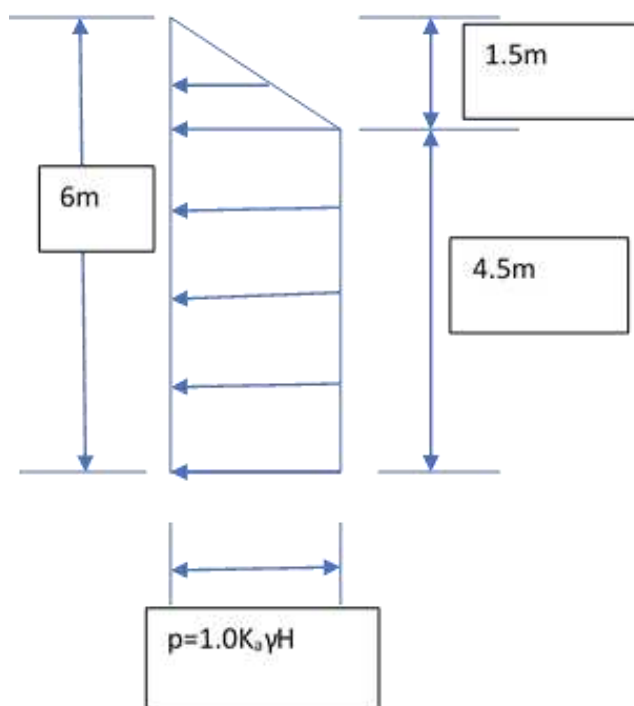


*Figure 24. Theoretical calculation of soil pressure on the trench box wall using the TPM equation.*

*Table 5. Experimental vs. theoretical and field performance soil pressures at different trench depths in soft clay soil.*

| Depth from top of the soil (m) | Maximum experimental stress (kPa) | Calculated total active stress from Rankine (1857): $P= 0.5\ (\gamma.H^2 - 4S_uH)$ (kPa) | Calculated stress from Terzaghi and Peck (1967): $p_A$=1.0 $K_A.\gamma.H$ (kPa) | Calculated stress from Yokel (1980): $p=We\ (H+2)$ (kPa) | Field performance data by LaBaw (2009): Maximum experimental strut load (kPa) |
|---|---|---|---|---|---|
| 0 | 0 | 0 | 0 | 75.69 | 0 |
| 0.9 | 6 | 12.69 | 26.4 | 75.69 | 71 |
| 2.4 | 23 | 33.84 | 44 | 75.69 | 67 |
| 3.9 | 114 | 56 | 44 | 75.69 | Not available due to experimental depth |
| 5.4 | 77 | 76.14 | 44 | 75.69 | Not available due to experimental depth |

*Note: H = 5.4 m for above calculated stresses.*
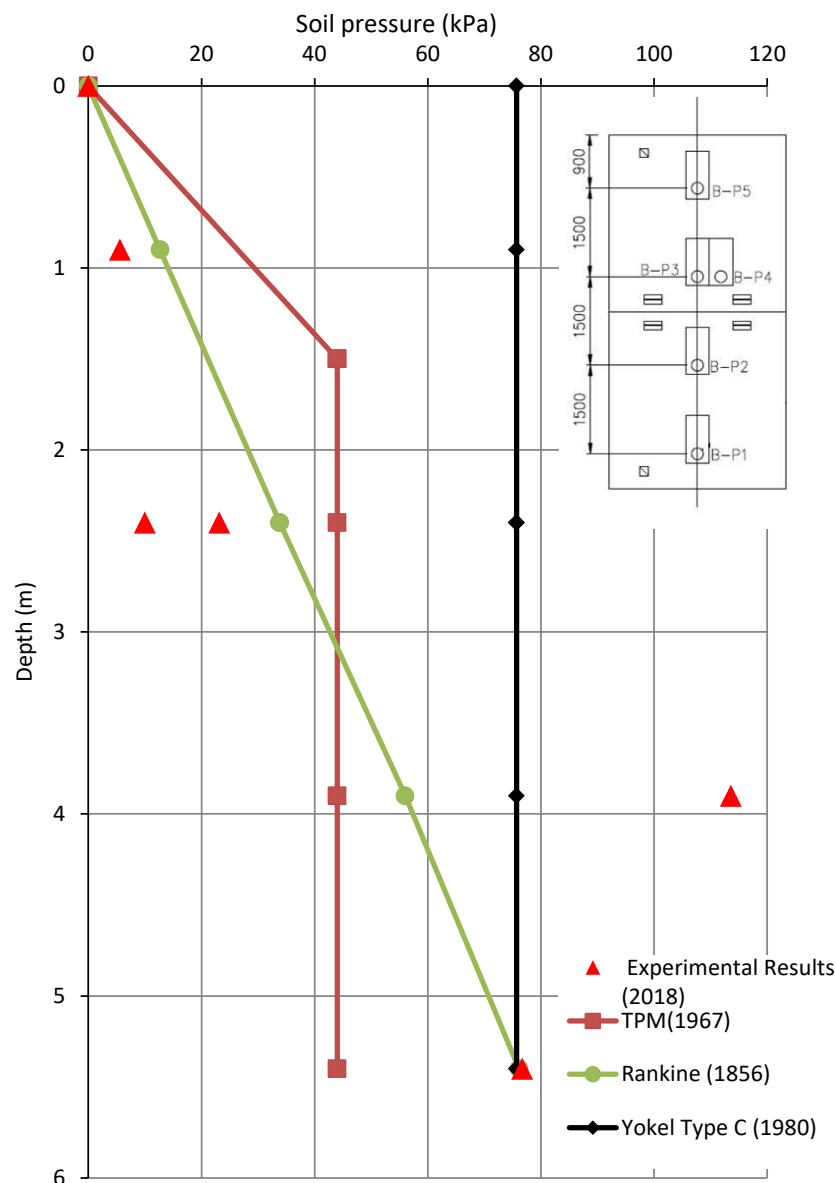
*Figure 25. Experimental vs. theoretical soil pressure curves with respect to trench depth.*

## CONCLUSIONS

The main objective of the field experimental work was to evaluate the soil pressure on the steel cage (Pro-tech, Pro 4 10 10) trench box at shallow depth in a sensitive clay trench. The study included two steel trench boxes stacked upon each other and assembled using "hinge connections" to cover the total depth of the 6 m (20 ft) trench in sensitive clay soil. Concrete blocks (representing a 45 kPa surcharge load) were installed very close to the trench to produce an extreme load case on the flexible wall of the trench box. Soil pressures were captured by total pressure cells (TPC) using vibrating-wire transducer technology. Based on the results of this study, the following observations can be made:

- Soil temperature variations were more pronounced in the upper part of the trench than in the deeper part.

- The deeper pressure cells in the trench experienced higher pressures (kPa) than the upper pressure cells. The maximum pressure was 114 kPa (2.38 ksf) at 3.9 m (12.8 ft) from the top.

- The effect of an overload applied close to the trench was more pronounced on the upper part of the trench box than on the deeper part. It followed that the pressure cells at 0.9 m and 2.4 m depths were more influenced by the 45 kPa overload in a short period of time. This reveals the need to maintain the minimum distance of 1.2 m (4 ft) from the excavation when stacking up any materials, in compliance with OSHA and SCCI guidelines.

- Theoretical calculations by Rankine (1857), Terzaghi and Peck (1967), and Yokel (1980) for this type of sensitive clay were compared with the pressures obtained from the field test results. Compared to Terzaghi and Peck, analytical values predicted by the Rankine and Yokel formulae were closer to experimental values. In terms of soil pressure along the depth of trench, in general, the analytical formulae underestimated the experimental values for the type of sensitive clay considered in this study.

## ACKNOWLEDGMENTS

## REFERENCES

Benmebarek, N., Labdi, H. and Benmebarek, S. (2016). "A Numerical Study of the Active Earth Pressure on a Rigid Retaining Wall for Various Modes of Movements." *Soil Mech. Found. Eng.*, 53, 39–45.

Bjerrum, L., Clausen, C. J. F., and Duncan, J. M. (1972). "Earth pressures on flexible structures; state-of-the-art report." *Proc., 5th European Conf. on Soil Mechanics Foundations Engineering*, Madrid, Spain, 169 –196.

Canadian Geotechnical Society, (2006). *Canadian Foundation Engineering Manual,* 4th edition.

Dourlet, S., (2020). *Étude expérimentale de deux excavations à Louiseville*, M. Sc. thesis, Québec: Université Laval.

Flaate, K. S., (1966). *Stresses and movements in connection with braced cuts in sand and clay*, Thesis report for Doctor of Philosophy in Civil Engineering, Urbana: Graduate College, University of Illinois.

Hashash, Y. M. A., and Whittle, A. J. (2002). "Mechanisms of load transfer and arching for braced excavations in clay." *J. Geotech. Geoenviron. Eng.,* 128, 187–197.

Henkel, D. J., (1971). "The calculation of earth pressures in open cuts in soft clays". *The Arup Journal*, 6(4), 14–15.

Karlsrud, K., and Andresen, L. (2005). "Loads on Braced Excavations in Soft Clay." *Int. J. Geomech.*, 5(2), 107-113.

LaBaw, S. M., (2009). *Earth Pressure Determination in Trench Rescue Shoring Systems*, Thesis report for Doctor of Philosophy, College Park: University of Maryland.

Lan, A., Arteau, J., LeBoeuf, D., Chaallal, O., and Dugré, J.M., (1999). "Conception d'un étançonnement adapté aux excavations en milieu urbain, Phase 2." Montreal: Institut de recherche Robert-Sauvé en santé et en sécurité du travail (IRSST). <https://www.irsst.qc.ca/en/ohs-research/research-projects/project/i/2207/n/conception-d-un-etanconnement-adapte-aux-excavations-en-milieu-urbain-0095-8360>.

Lefebvre, G. (1981). "Fourth Canadian Geotechnical Colloquium: Strength and slope stability in Canadian soft clay deposits." *Can. Geotech. J.*, 18(3), 420-442.

Leroueil, S., Hamouche, K., Tavenas, F., Boudali, M., Locat, J., Virely, D., Roy, M., La Rochelle, P.,and Leblond, P., (2003). "Geotecnical characterization and properties of a sensitive clay from Québec." *Characterisation and Engineering Properties of Natural Soil,* T.S. Tan. et al., eds, Lisse: Swets & Zeitlinger, 363-393.

Macnab, A., (2002). *Earth Retention Systems Handbook*, New York: McGraw-Hill.

Mortensen, N., and Andresen, L. (2003). "Analysis of undrained excavation in anisotropic clay." *Proc., Int. Workshop on Geotechnics of Soft Soils Theory and Practice—SCMEP*, Noordwijkerhout, The Netherlands, 245–250.

National Research Council Canada, (2015). *National Building Code of Canada*, Commentary K. Ottawa, Ontario.

OSHA, (2015). *OSHA Technical Manual (OTM)*, Directive Number: TED-01-00-015, Section V, Chapter 2: Excavations: Hazard Recognition in Trenching and Shoring. Washington, DC: U.S. Department of Labor. <https://www.osha.gov/dts/osta/otm/otm_v/otm_v_2.html>.

Rankine, W., (1857). "On The Mathematical Theory of The Stability of Earth-work and Masonry". *London, The Royal Society of London*. 9-27.

Rochelle, P. L., Sarrailh, J., Tavenas, F., Roy, M., and Leroueil, S. (1981). "Causes of sampling disturbance and design of a new sampler for sensitive soils." *Can. Geotech. J.*, 18(1), 52-66.

Roctest, (2005*). Instruction Manual, Vibrating-Wire Pressure Cells, Model TPC & EPC*, 19-21.

SCCI, (2020). *Safety Code for the Construction Industry*, Quebec: Government of Quebec, <http://legisquebec.gouv.qc.ca/en/ShowDoc/cr/S-2.1,%20r.%204>.

Terzaghi, K. and Peck, R. B., (1967). *Soil Mechanics in Engineering Practice*, 2nd Ed., Wiley, New York.

Yokel, F. Y., Tucker, L. R., and Reese, L. C., (1980). *Soil Classification for Construction Practice in Shallow Trenching*, Washington, DC: National Bureau of Standards. 1-96.

# INTERNATIONAL JOURNAL OF GEOENGINEERING CASE HISTORIES